Luminance-contrast properties of texture-shape and texture-surround suppression of contour shape

Elena Gheorghiu

Department of Psychology, University of Stirling, Stirling, Scotland, United Kingdom

Frederick A. A. Kingdom

Department of Ophthalmology, McGill Vision Research, McGill University, Montreal, QC, Canada

Studies have revealed that textures suppress the processing of the shapes of contours they surround. One manifestation of texture-surround suppression is the reduction in the magnitude of adaptation-induced contour-shape aftereffects when the adaptor contour is surrounded by a texture. Here we utilize this phenomenon to investigate the nature of the first-order inputs to texture-surround suppression of contour shape by examining its selectivity to luminance polarity and the magnitude of luminance contrast. Stimuli were constructed from sinusoidal-shaped strings of either "bright" or "dark" elongated Gaussians. Observers adapted to pairs of contours, and the aftereffect was measured as the shift in the apparent shape frequency of subsequently presented test contours. We found that the suppression of the contour-shape aftereffect by a surround texture made of similar contours was maximal when the adaptor's center and surround contours were of the same polarity, revealing polarity specificity of the surround-suppression effect. We also measured the effect of varying the relative contrasts of the adaptor's center and surround and found that the reduction in the contour-shape aftereffect was determined by the surround-to-center contrast ratio. Finally, we measured the selectivity to luminance polarity of the texture-shape aftereffect itself and found that it was reduced when the adaptors and tests were of opposite luminance polarity. We conclude that texture-surround suppression of contour-shape as well as texture-shape processing itself depend on "on–off" luminance-polarity channel interactions. These selectivities may constitute an important neural substrate underlying efficient figure–ground segregation and image segmentation.

Introduction

Contours and textures play an important role in object recognition; contours provide information about the shapes of objects, and textures are useful for figure–ground segmentation and surface shape perception (Biederman, 1987; Julesz, 1981; A. Li & Zaidi, 2000; Malik & Perona, 1990; Marr, 1982). In natural scenes, objects are often surrounded by other objects or set against textured backgrounds. Studying how the human visual brain processes the shapes of objects when surrounded by textures is important for a full understanding of object recognition and texture perception.

Textures can modulate our perception of the shapes of contours they surround (Gheorghiu & Kingdom, 2012a, 2012b; Gheorghiu, Kingdom, & Petkov, 2014; Grigorescu, Petkov, & Westenberg, 2003, 2004; Kingdom & Prins, 2009; Z. Li, 1999, 2002; Petkov & Westenberg, 2003). One such contextual effect is the effect of a surround texture on a particular shape aftereffect: the shift in the apparent shape frequency and shape amplitude of a sinusoidal-shaped contour following adaptation to a differently shaped sinusoidal contour (Gheorghiu & Kingdom, 2006, 2008, 2009). When the adapting contour is surrounded by a texture made of a series of identical contours arranged in parallel, the shape aftereffect is reduced even though the surround contours in the adapting stimulus have potential adaptive power. We have termed this phenomenon *texture-surround suppression of contour shape* or TSSCS (Gheorghiu & Kingdom, 2011; Gheorghiu, Kingdom, Thai, & Sampasivam, 2009; Kingdom & Prins, 2009). Gheorghiu, Kingdom, and Petkov (2014) proposed that this type of contextual influence reflects a general-purpose mechanism that "detexturizes" an image by enhancing the representation of isolated contours at the expense of contours that are embedded in textures. In other words, contours that are part of textures are prevented from contributing to object-shape perception while continuing to contribute to texture-shape perception.

In this communication, we examine whether TSSCS as well as texture-shape perception itself exhibit

Citation: Gheorghiu, E., & Kingdom, F. A. A. (2019). Luminance-contrast properties of texture-shape and texture-surround suppression of contour shape. *Journal of Vision*, *19*(12):4, 1–14, https://doi.org/10.1167/19.12.4.

https://doi.org/10.1167/19.12.4 Received June 26, 2019; published October 15, 2019 ISSN 1534-7362

selectivity to luminance contrast polarity (henceforth, just luminance polarity) as well as selectivity to luminance contrast.

Our motivation for examining the role of luminance polarity in TSSCS concerns recent contradictory evidence on the role of luminance polarity in contour and texture processing. Studies of shape aftereffects obtained with single contour adaptors and tests have shown selectivity to luminance polarity in that when the adaptor and test contours differ in luminance polarity, the aftereffect is reduced (Bell, Gheorghiu, Hess, & Kingdom, 2011; Gheorghiu & Kingdom, 2006). With textures, however, results are more equivocal. On the one hand, Motoyoshi and Kingdom (2007) showed that modulations of texture orientation (although not contrast modulation) were detected by mechanisms that indiscriminately pool signals of different luminance polarity. On the other hand, studies have shown that humans can discriminate textures based on differences in the contrast polarities of their texture elements (Chubb, Econopouly, & Landy, 1994; Hansen & Hess, 2006; Malik & Perona, 1990; Rentschler, Hubner, & Caelli, 1988). It is, therefore, an open question as to whether with TSSCS a difference in luminance polarity between the adaptor's central contour and its multi-contour texture surround serves to lessen the (negative) impact of the surround on the shape aftereffect.

Turning now to the question of selectivity to luminance contrast, previous studies have shown that tilt aftereffects induced by very brief adaptation saturate rapidly at low contrast, implying broad tuning to contrast (Suzuki, 2001). On the other hand, the tilt illusion, in which the apparent orientation of a central-grating stimulus is altered by the presence of a differently oriented grating surround, shows selectivity to the relative contrast between center and surround (Durant & Clifford, 2006; Qiu, Kersten, & Olman, 2013; Tolhurst & Thompson, 1975). Weak selectivity to contrast has been shown for contour-shape aftereffects (Gheorghiu & Kingdom, 2006) and figural aftereffects for faces (Yamashita, Hardy, De Valois, & Webster, 2005). The selectivity to contrast found in adaptation studies has been attributed to contrast-gain control mechanisms that are known to be a canonical feature of cortical neural function (Bonds, 1989, 1991; Heeger, 1992; Ohzawa, Sclar, & Freeman, 1982, 1985). Studies of texture processing have shown that humans can segregate texture regions based solely on differences in contrast (Kingdom, Prins, & Hayes, 2003; Motoyoshi & Kingdom, 2007; Prins & Kingdom, 2002; Sutter, Sperling, & Chubb, 1995). On these grounds, we might expect TSSCS to be, to some extent, selective to luminance contrast.

In the three experiments described below, we examine whether TSSCS and texture–shape aftereffects are tuned to luminance polarity and contrast. To do this, we have measured shape aftereffects for contours and textures composed of strings of either elongated Gaussian or Gabor elements. For TSSCS, we compare contour-shape aftereffects for center-contour and surround-texture adaptors defined along either the same or different luminance polarities/contrasts. For texture shape, we compare aftereffects between same and different adaptor luminance polarities/contrasts. The results of this study have enabled us to refine our understanding of the role of luminance polarity and contrast in contextual effects on contour-shape and texture-shape processing.

Methods

Participants

Eleven observers participated in this study: one of the two authors (who took part only in Experiment 1) and 10 observers who were naive with regard to the experimental aims. Five observers took part in Experiments 1 and 3 and three in Experiment 2. All observers had normal or corrected-to-normal visual acuity. Observers gave their written informed consent prior to participating in this study and were treated in accordance with the Declaration of Helsinki (2008, version 6). All research procedures were approved by the University of Stirling Ethics Committee.

Stimuli: Generation and display

The stimuli were generated by a ViSaGe MKII video-graphics card (Cambridge Research Systems Ltd., UK) with 12 bits contrast resolution and presented on a gamma-corrected 20-in. ViewSonic Professional Series PF817 cathode ray tube monitor (ViewSonic, Brea, CA) with spatial resolution of 1,024 $\times$ 768 and refresh rate of 85 Hz. The R (red), G (green), and B (blue) outputs of the monitor were gamma-corrected after calibration with an Optical OP200E photometer. All stimuli were presented in the center of the monitor on a midgray background with mean luminance of 47.2 cd/m^2. Viewing distance was 100 cm.

Adapting stimuli were pairs of sinusoidal-shaped textures and contours made of strings of elongated Gaussians (Experiments 1 and 2) or strings of Gabor elements (Experiment 3) presented in the center of the monitor on the average luminance background and located 4° above and below the fixation marker as shown in Figure 1a and d, respectively. Textures were made of a series of 19 contours arranged in parallel and were shown in a rectangular window of 9° $\times$ 7°. The

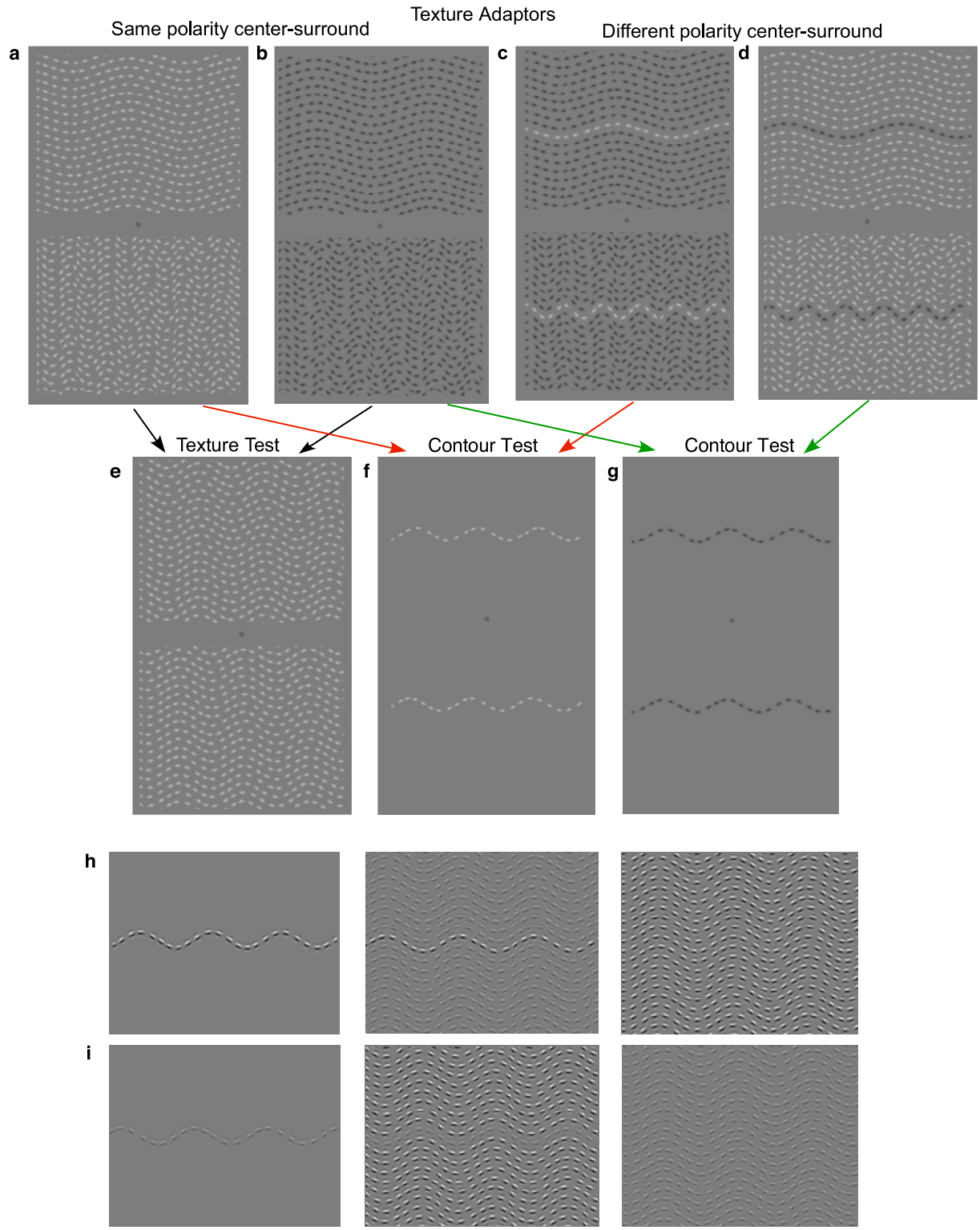

Figure 1. Stimuli used in the experiments. One can experience the shape-frequency aftereffect by fixating between the pair of adapting textures (a–d) for about 90 s and then shifting one's gaze to the marker placed between the pair of (a) test-textures or (f and g) single test contours. The texture adaptors consisted of a central contour flanked by (a and b) same-polarity surround, i.e., center and surround both white or black and (c and d) different-polarity surround, i.e., white center flanked by black surround and black center flanked by white surround. For the texture-shape aftereffect, the test stimuli were test texture (e). For the contour-shape aftereffect, the test stimuli were pairs of single contours of the same luminance polarity as the central-contour adaptor (f and g). (h and i) Example stimuli used in Experiment 3: (h) high-contrast and (i) low-contrast single contour (left panels) flanked by different (middle panels) and same (right panels) contrast texture surround.

adapting pair consisted of textures or contours with shape frequencies of 0.2 and 0.6 c/°, giving a geometric mean shape frequency of 0.35 c/°. The mean shape frequency of the test texture pair (Experiment 1) and test contour pair (Experiments 2 and 3) were held constant at 0.35 c/°. The shape amplitude of the two adaptors and tests was always fixed at 0.3°.

In Experiments 1 and 2, the contours and textures were made of elongated Gaussian micropatterns. The luminance profile of the Gaussian perpendicular to its major axis had a sigma of 0.08°. The center-to-center spacing between adjacent micropatterns along the path of the line was 0.45°. The luminance contrast of each micropattern was set at 90% Michelson contrast with +90% for "white" and −90% for "black."

In Experiment 1, we examined whether texture shapes are selective to luminance polarity. To do so, we used texture adaptor and texture test patterns that were either the same or different in luminance polarity. There were four adaptor-test conditions: adaptor and test both white (Figure 1a and e), adaptor and test both black, adaptor white and test black, and adaptor black and test white (Figure 1b and e).

In Experiment 2, we examined whether texture-surround suppression of contour shape is selective to luminance polarity. To do this, we used a texture adaptor in which central contour and surround were either the same (Figure 1a and b) or different in luminance polarity (Figure 1c and d). We used three adapting conditions: central contour only (or no surround), contour flanked by same-polarity surround (i.e., center and surround both white or black), and contour flanked by different-polarity surround (i.e., white center flanked by black surround and black center flanked by white surround). The test stimuli were single contours of the same luminance polarity as the central contour adaptor (Figure 1f and g). We measured shape aftereffects for all six adaptor test combinations (2 polarities × 3 center-surround adaptor combinations).

In Experiment 3, all contours were constructed from strings of odd symmetric (d.c. balanced) Gabor patches with a spatial bandwidth of 1.75 octaves and a center luminance spatial frequency of 5 c/°. The Gabor patches were positioned along the sinusoidal-shaped profile and were oriented tangentially to the path of the contour. The center-to-center spacing between adjacent Gabor patches along the contour was randomly selected from within the range ±0.15° around a mean of 0.45°. On average, there were 22 Gabors per contour, but because the Gabor strings were contained within a fixed width window, the number of Gabors differed between the pair of adaptors by a factor of 1.25 with 20 Gabors for the low and 25 Gabors for the high shape-frequency contours.

The texture adaptors consisted of a central contour flanked by a surround made of nine parallel contours. We varied the contrast of both center contour and texture-surround adaptors. We used three contrast values: 0.1, 0.3, and 0.9. This resulted in nine combinations of center and surround contrasts (3 center × 3 surround contrasts) and three no-surround contrast conditions, thus leading to 12 conditions in total. Example center-surround adaptor stimuli are shown in Figure 1h and i. In all conditions, the contrast of the test contour was always the same as the contrast of the central contour adaptor.

Procedure: Shape aftereffects

Adapting stimuli consisted of pairs of sinusoidal-shaped textures or contours as shown in Figure 1. The test stimuli were pairs of textures (Experiment 1) or pairs of single contours (Experiments 2 and 3).

Each session began with an initial adaptation period of 90 s, followed by a repeated test of 0.5 s duration interspersed with top-up adaptation of 2.5 s. During the adaptation period, the shape phase of the contour or texture was randomly changed every 0.5 s in order to prevent the formation of afterimages and to minimize the effects of local orientation adaptation. An important property of shape-frequency aftereffect is that the aftereffect survives shape-phase randomization during adaptation as can be experienced in the nonstatic, contour adaptor; an example is shown in Supplementary Movie S1. The presentation of each test contour or test texture was signaled by a tone. Subjects were required to fixate on the marker placed between each pair of contours for the entire session.

A staircase method was used to estimate the point of subjective equality (PSE). The geometric mean shape frequency of the two test contours (Experiments 1 and 2) or test textures (Experiment 3) was held constant at 0.35 c/° during the test period while the computer varied the relative shape frequencies of the two test contours or textures in accordance with the subject's response. At the start of the test period, the ratio of the two test shape frequencies was set to a random number between 0.7 and 1.44. On each trial, subjects indicated via a button press whether the upper or lower test contour (Experiments 1 and 2) or test textures (Experiment 3) had the higher perceived shape frequency. The computer then changed the ratio of test shape frequencies by a factor of 1.06 for the first five trials and 1.015 thereafter in a direction opposite to that of the response, i.e., toward the PSE. The session was terminated after 25 trials. In order that the total amount of adaptation for each condition was the same, we used a staircase method that was terminated after a fixed number (25) of trials rather than a fixed number

of reversals. We found in previous studies (Gheorghiu & Kingdom, 2006, 2008, 2009; Gheorghiu, Kingdom, Bell, & Gurnsey, 2011; Gheorghiu, Kingdom, & Witney, 2010) that a step size of 1.015 was sufficient to produce a visible change in the shape frequency on each trial while ensuring a stable convergence over the last 20 trials and, hence, an accurate estimate of the PSE. The shape-frequency ratio at the PSE was calculated as the geometric mean shape-frequency ratio of the two tests (with the ratio's numerator the test at the position of the lower shape-frequency adaptor and its denominator the test at the position of the higher shape-frequency adaptor) averaged across the last 20 trials.

For each with-adaptor condition, we made six measurements: three in which the upper adaptor had the higher shape frequency and three in which the lower adaptor had the higher shape frequency. In addition, we measured for each condition the shape-frequency ratio at the PSE in the absence of the adapting stimulus (i.e., the no-adaptor condition). To obtain an estimate of the size of the shape aftereffect, we first calculated the difference between the logarithm of each with-adaptor shape-frequency ratio at the PSE and the mean of the logarithms of the no-adaptor shape-frequency ratios at the PSE. We then calculated the mean and standard error of these differences across the six measurements. These standard errors are the ones shown in the graphs. Note that the magnitude of the aftereffect is defined as the ratio of shape frequencies at the PSE, and thus, its units are dimensionless.

Experiments and results

Experiment 1: Is texture shape selective to luminance polarity?

Here, we measured the shape aftereffect for *texture* adaptors and *texture* tests. All combinations of same and different luminance polarity adaptor and tests were tested. Figure 2 shows the aftereffects obtained with same (white and black bars) and different (light and dark gray bars) texture adaptor/test polarity combinations for five observers (Figure 2a) and for the average across observers (Figure 2b). The aftereffects normalized to the mean same-polarity adaptor/test conditions are shown in Figure 2c. Different-polarity conditions produced significantly smaller aftereffects than same-polarity conditions (compare white and black bars with light/dark gray bars). The transfer of aftereffect across different polarities was about 0.36, indicating that the texture-shape aftereffect is partially selective to luminance polarity.

To determine whether the luminance polarity selectivity was significant, we performed a two-way, repeated-measures ANOVA with factors Adaptor-Test Combination (same vs. different) and Test Polarity (white vs. dark) on the observers' aftereffect data (Figure 2a). The analysis revealed a significant main effect of Adaptor-Test Combination, $F(1, 4) = 26.1$, $p = 0.007$, $\eta_p^2 = 0.867$, indicating that the aftereffect is selective to luminance polarity. Bonferroni-corrected pairwise comparisons (paired-samples t tests) showed significant differences between all same versus different conditions (all ps < 0.03). The main effect of test polarity, $F(1, 4) = 0.172$, $p = 0.699$, $\eta_p^2 = 0.041$, and the interaction effect, $F(1, 4) = 0.002$, $p = 0.969$, $\eta_p^2 = 0.000$, were found not significant.

Experiment 2: Is texture-surround suppression of contour shape selective to luminance polarity?

Here we examine whether TSSCS is selective to luminance polarity. To do this, we used three adapting conditions: single contour, i.e., no surround; contour flanked by surround of the same luminance polarity (Figure 1a and b); and contour flanked by surround of different luminance polarity (Figure 1c and d). The test stimuli were all single contours of the same luminance polarity as the central contour adaptor (Figure 1f and g). We measured shape aftereffects for all six adaptor-test combinations (2 polarities $\times$ 3 center-surround adaptor combinations).

Figure 3a shows the aftereffects obtained with adaptor contours flanked by same-polarity surrounds (white and black bars), different-polarity surrounds (light/dark gray bars), or no surround (red dashed line) for three observers and for the average across observers. These results show that the effect of both same and different polarity surrounds is to reduce the aftereffect from its no-surround baseline (compare bars with red dashed line) and that the reduction is greater when the center and surround contours are of the same compared to different polarity (compare light/dark gray and white/black bars in Figure 3a). We also express the results in terms of the magnitude of surround suppression by calculating a surround suppression index (SSI) as follows: $SSI = 1 - SFAE_{with\ surround}/SFAE_{no\ surround}$, where $SFAE_{with\ surround}$ and $SFAE_{no\ surround}$ are the shape-frequency aftereffects obtained with and without the surround texture, respectively. The SSI is inversely related with the magnitude of the aftereffect. Hence, an SSI of one indicates complete suppression of the aftereffect, and an SSI of zero indicates no suppression. Figure 3b plots the across-observers mean SSI for each center-surround polarity condition (left panel) averaged across all same versus opposite polarity conditions (right panel). The results show that texture-surround suppression is only weakly selective for surround luminance

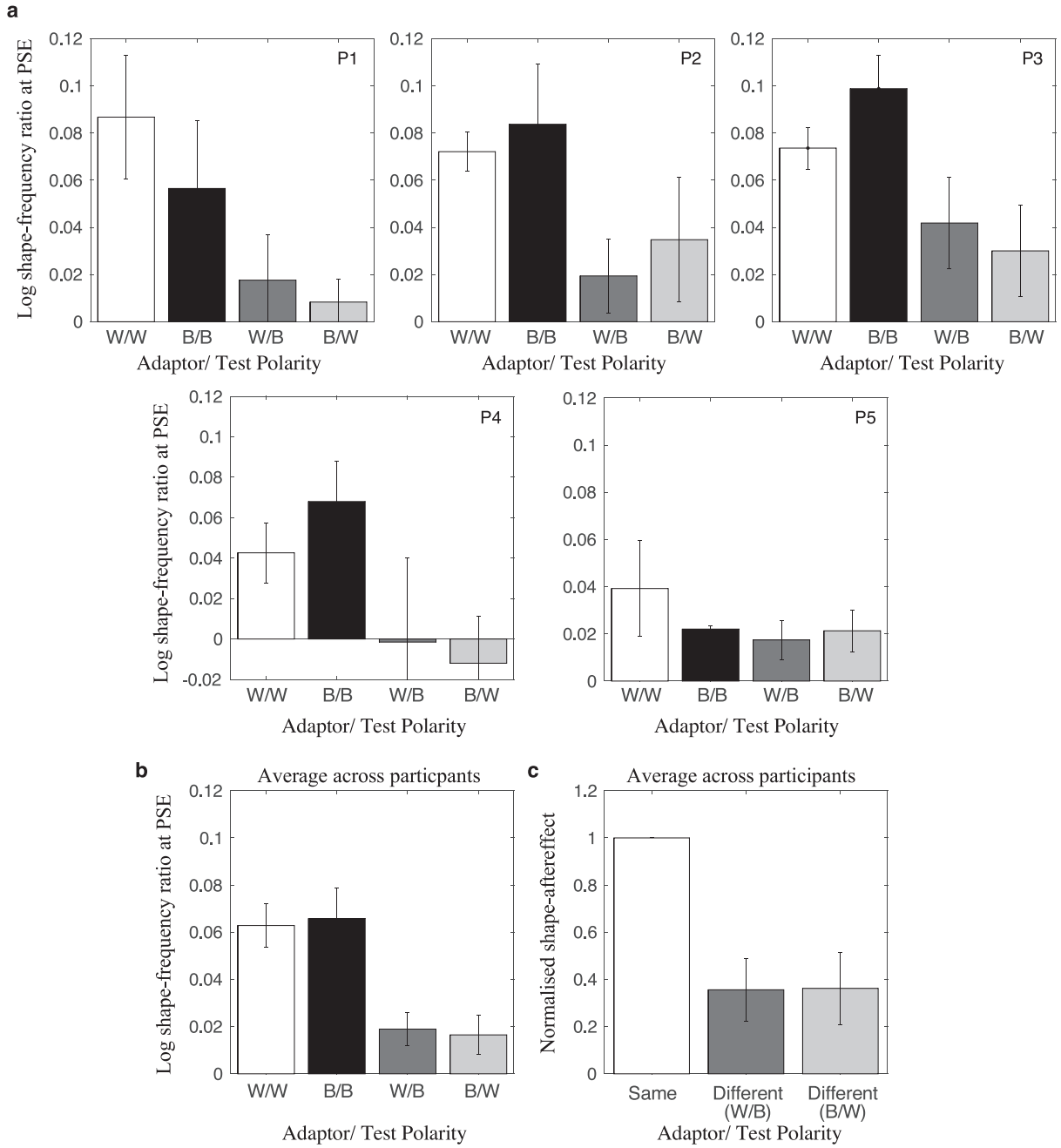

Figure 2. Results of Experiment 1. Texture-shape aftereffects for adaptor-test combinations with the same and opposite luminance polarity for (a) the five observers and (b) the average across observers. Different types of textures are indicated as follows: W = white and B = black. W/B means white texture-adaptor and black test-texture. Same polarity conditions W/W and B/B are shown as white and black bars, respectively. Different-polarity conditions W/B and B/W are indicated by dark/light gray bars. (c) The texture-shape aftereffects normalized to the mean same-polarity adaptor/test conditions.

polarity with an average SSI of 0.73 for same-polarity and 0.48 for different-polarity surrounds, a difference of about 25%.

To determine whether the luminance polarity selectivity of TSSCS was significant, a two-way repeated-measures ANOVA with factors Center-Surround polarity combination (same vs. different) and Polarity of central contour adaptor/test (white vs. dark) was performed on the aftereffect data shown in Figure 3a. The main effect of Center-Surround polarity combination was significant, $F(1, 2) = 107.309$, $p = 0.009$, $\eta_p^2 = 0.982$, indicating that the aftereffect is selective for the surround polarity. The main effect of the central contour adaptor/test polarity was found not significant,

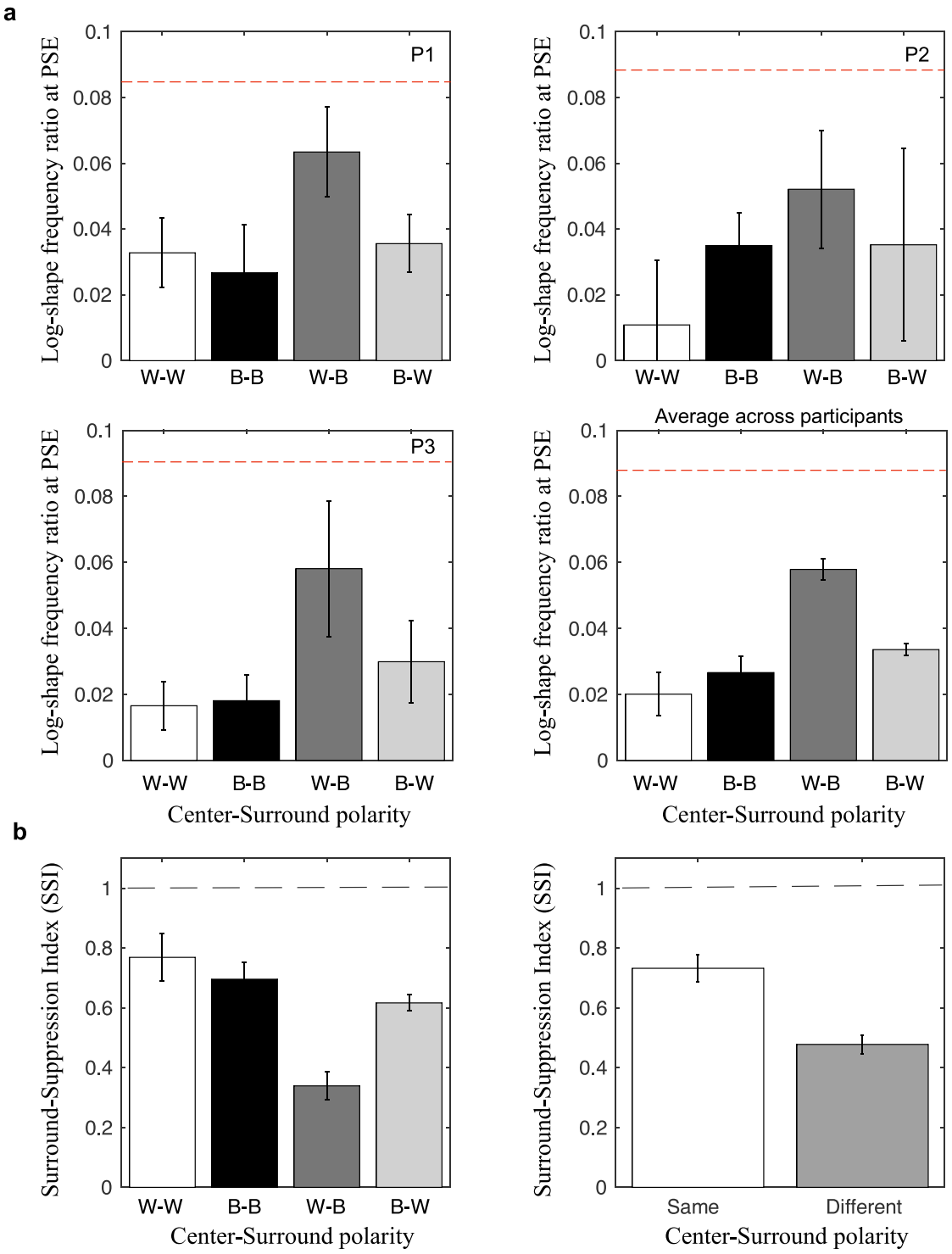

Figure 3. Results of Experiment 2. (a) Contour-shape aftereffects obtained using texture adaptor and contour test in which the central-contour adaptor was flanked by same-polarity texture surrounds (white and black bars), different-polarity texture surrounds (light and dark gray bars), and no surround (red dashed line). Different types of stimuli are indicated as follows: W = white and B = black. B-W means black central contour flanked by white surround. (b) Across-observers mean SSI for each center-surround polarity condition (left) and averaged across all same versus opposite polarity conditions (right). Note that SSI is inversely related with the magnitude of the aftereffect. A surround suppression index of one indicates complete suppression, and zero indicates complete lack of suppression.

$F(1, 2) = 1.973$, $p = 0.295$, $\eta_p^2 = 0.497$. However, there was a significant interaction between Center-Surround polarity combination and Polarity of central contour adaptor/test, $F(1, 2) = 30.27$, $p = 0.031$, $\eta_p^2 = 0.938$. Pairwise comparisons (paired-samples t tests) showed that the interaction was driven by the white-center/black-surround condition, which was significantly different from the white-center/white-surround, $t(2) = 10.54$, $p = 0.009$; black-center/black-surround, $t(2) = 4.375$, $p = 0.048$; and black-center/white-surround, $t(2) = 6.564$, $p = 0.022$, conditions. However, after Bonferroni correction none of the pairwise comparisons were significant ($p > 0.05$).

Experiment 3: Does TSSCS depend on the contrast of the surround?

In this experiment, we investigated the effect of the relative contrast of the surround on the suppression of the contour-shape aftereffect. To do this, we varied the contrast of the center adaptor contour as well as its texture surround. We used three contrast values: 0.1, 0.3, and 0.9, which resulted in nine combinations of center and surround contrasts (3 center × 3 surround contrasts) along with three no-surround contrast conditions.

Figure 4 shows the size of the shape aftereffect for five observers plotted as a function of the contrast of the adaptor's texture surround for low (Figure 4a), intermediate (Figure 4b), and high (Figure 4c) contrast of the center contour adaptor, with the central-contour adaptor and test contrast indicated by the red arrows. The dashed lines indicate the size of the aftereffect obtained with a no-surround adaptor. Although in some of the observers, the biggest reduction in the aftereffect occurs when surround and center contours have the same contrast (as when the aftereffect indicated by the red arrow is the lowest of the three values in a plot), this is not consistent across observers.

Figure 5 plots the across-observers average SSI as a function of surround contrast (Figure 5a) and surround-to-center contrast ratio (Figure 5b). The most telling plot is that of Figure 5b, which reveals the effect on the SSI of the surround-to-center contrast ratio. To determine whether the effect of contrast of TSSCS was significant, we performed a two-way repeated-measures ANOVA on the data shown in Figure 4 with factors Center contrast (0.1 vs. 0.3 vs. 0.9) and Surround contrast (0.1 vs. 0.3 vs. 0.9). The analysis revealed a significant main effect of center contrast, $F(2, 8) = 83.165$, $p < 0.0001$, $\eta_p^2 = 0.954$, and surround contrast, $F(2, 8) = 5.646$, $p = 0.03$, $\eta_p^2 = 0.585$, and no significant interaction effect, $F(4, 16) = 2.306$, $p = 0.103$, $\eta_p^2 = 0.366$. In sum, this experiment indicates that the strength of surround suppression increases with surround-to-center contrast ratio (Figure 5b).

Discussion

We have examined whether texture-shape and texture-surround suppression of contour shape are tuned to luminance polarity and to the magnitude of luminance contrast. Our results indicate that (i) texture-shape aftereffects are selective for luminance polarity, (ii) TSSCS shows weak selectivity for luminance polarity, and (iii) TSSCS increases with the surround-to-center contrast ratio. Thus, texture-shape processing and TSSCS appear to depend on the activity of ON and OFF luminance polarity channels, and TSSCS is sensitive to the relative contrasts of the surround texture and center contour. Our results complement previous findings showing selectivity to luminance polarity for other visual dimensions, e.g., illusory contour perception (He & Ooi, 1998) and the luminance spatial frequency aftereffect (Blake, Overton, & Lema-Stern, 1981; Blakemore & Sutton, 1969; Burton, Nagshineh, & Ruddock, 1977; De Valois, 1977a, 1977b; Fiorentini, Baumgartner, Magnussen, Schiller, & Thomas, 1990) although, interestingly, not the tilt aftereffect (Gheorghiu, Bell, & Kingdom, 2013; Magnussen & Kurtenbach, 1979).

Our first finding, namely that the texture-shape aftereffect is selective to luminance polarity is, at first sight, at odds with Motoyoshi and Kingdom's (2007) findings with orientation-defined texture perception. They found that the detection of modulations of texture orientation was agnostic to variations in luminance polarity, implying that the mechanisms involved indiscriminately pooled signals of opposite luminance polarity. The most likely reason for this discrepancy is that texture-shape perception and texture-modulation detection are different tasks mediated by different neural mechanisms. It is widely believed that texture modulation detection is mediated by a relatively low-level process that detects variations in contrast energy within narrowband spatial-frequency and orientation-selective channels, as modeled, for example, by the filter-rectify-filter cascade (Graham, 2011; Landy, 2013). Given a task emphasis on modulation *detection*, it might arguably make sense for vision to indiscriminately summate signals across luminance polarity. On the other hand, given a task emphasis on texture *shape* perception, important as it is for object and surface-shape recognition, it might be more prudent for vision to preserve local feature properties, such as luminance polarity.

This explanation does not, however, square with our previous findings using a similar protocol but with

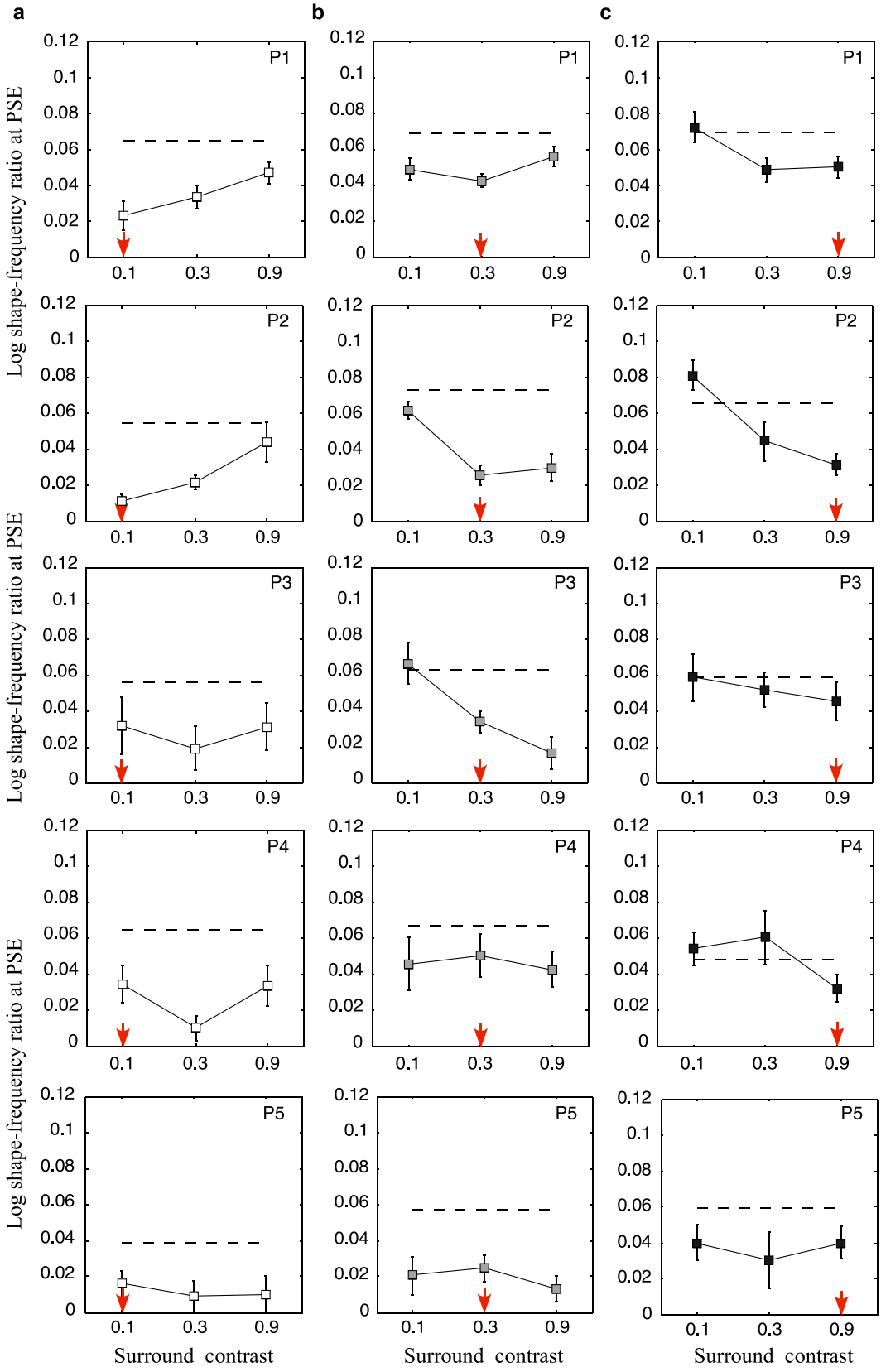

Figure 4. Results of Experiment 3. The contour-shape aftereffect plotted as a function of the contrast of the adaptor's texture surround for low (a), intermediate (b), and high (c) contrast of the center-contour adaptor, with the central-contour adaptor and test contrast indicated by the red arrows. Dashed lines indicate the size of contour-shape aftereffects obtained with contour only (i.e., no surround) adaptors.

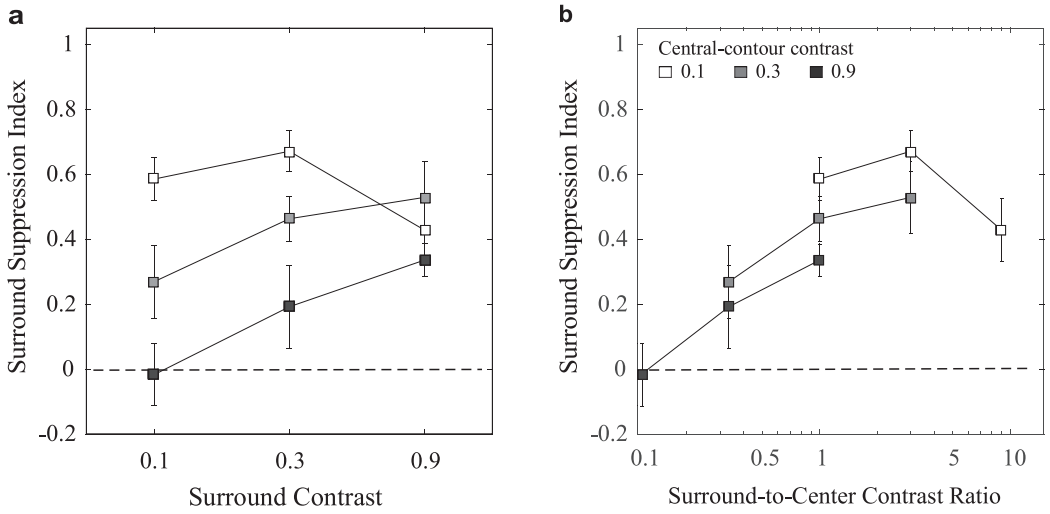

Figure 5. Results of Experiment 3. (a) Across-observers average surround suppression index (SSI) plotted as a function of the contrast of the adaptor's texture-surround, for low (white), intermediate (gray), and high (black) contrast of the center-contour adaptor. (b) SSI data plotted in terms of surround-to-center contrast ratio. Note that SSI is inversely related with the magnitude of the aftereffect. A surround suppression index of one indicates complete suppression, and zero indicates complete lack of suppression.

adaptors and tests made of Gabor elements and defined along same or different axes of cardinal color space (Gheorghiu and Kingdom, 2012a). We found no selectivity for the L–M (commonly termed red–green), S (commonly termed blue–yellow), and L + M (luminance) cardinal axes, where L, M, and S refer to the long-, medium-, and short-wavelength cones. In the current study, the adapting and test textures were made of elongated Gaussians defined along the same or opposite polarities *within* the luminance axis. Thus, it is possible that either our use of Gaussians rather than Gabors or the fact that the former isolated the individual poles of the luminance axis rather than just the axis itself is the reason for the difference in results found here compared to that of Gheorghiu and Kingdom (2012a).

As for TSSCS, Gheorghiu and Kingdom (2012a) found that TSSCS was only weakly selective to the cardinal axis of the surround texture when the central contour was defined along either the red–green or blue–yellow cardinal axes with an average SSI of ~0.68 for same-color and ~0.42 for different-color surrounds—thus, a difference of about 25%. Perhaps more germane to the present results was our finding of no selectivity to cardinal axis when the central contours were luminance defined. In the current study, surround suppression was weakly selective for luminance polarity (a difference in SSI of about 25% between same and different luminance polarity center-surround conditions, which is comparable with that found by Gheorghiu & Kingdom, 2012a, for color-defined central contours). Again, it is possible that the use of elongated Gaussian elements and/or the uses of axis poles rather than axes underpinned the differences in selectivity found with luminance-defined central contour in the two studies.

Our results (Experiment 2) hint also to an asymmetry in surround suppression obtained with different polarity center-surround conditions with weaker suppression by a black surround of a white center contour (0.34) than vice versa (0.62) (compare light and dark gray bars in Figure 3). What might cause this asymmetry? Asymmetries in the processing of increments and decrements are well known. For example, more neurons respond to black compared to white stimuli in area V1 (Xing, Yeh, & Shapley, 2010), an imbalance that has been invoked to explain the higher sensitivity to decrements than to increments (Shi & Shinomori, 2013). There are also increment–decrement differences in magnocellular pathway response dynamics (Ehrenstein & Spillmann, 1983; Komban, Alonso, & Zaidi, 2011; Rekauzke et al., 2016; Shi & Shinomori, 2013; Whittle, 1986). For example propagation speeds to V1 are higher for decrements than increments (Rekauzke et al., 2016) and latencies for detecting decrements are shorter than those for detecting increments (Komban et al., 2011; Komban et al., 2014). We know from our previous studies with TSSCS that, if the surround and center signals are temporally asynchronous by more than 100 ms, there is a significant reduction in the amount of surround suppression (Gheorghiu & Kingdom, 2017). Thus, it is possible that the asymmetry found here, namely less suppression from a black compared to a white surround (with opposite polarity centers), could be due to differences in increment–decrement signal arrival times in visual areas beyond V1 concerned with processing contour shape.

The differences in the findings of the present study and that of Gheorghiu and Kingdom (2012a) might also reflect the relative contribution of monocular and binocular neurons to the shape aftereffect. Evidence for this comes from another center-surround interaction effect, the tilt illusion, in which a center-surround difference along the chromatic-luminance dimension significantly reduced the illusion but only when the stimulus center and surround were presented monocularly/to the same eye (Forte & Clifford, 2005). However, when the center and surround were presented interocularly, the interocular transfer of the tilt illusion was almost complete, thus suggesting that the binocular component of the tilt illusion was not (or only weakly) selective to color. Thus, Forte and Clifford (2005) showed that the monocular component of the tilt illusion is color selective while the binocular component is not. Perhaps it might be the case that binocular spatial channels are less selective to cardinal axis and/or within-axis polarity than monocular spatial channels.

With this in mind, our previous studies suggest that contour shape effects obtained with single-contour adaptors and tests are mediated by binocular neurons as indicated by the substantial amount of interocular transfer of the aftereffects. Whichever binocular neurons are involved, however, they do not appear to be tuned to stereo-depth—the aftereffects were largely unchanged after placing the adaptor and test into a different stereo-depth plane (Gheorghiu et al., 2009). On the other hand, the suppression of the aftereffects by surround texture was maximal when the surround and center contours lay in the same depth plane, implying stereo-depth selectivity of TSSCS (Gheorghiu et al., 2009). It, therefore, may be that part of the reason for the weak albeit significant selectivity to luminance polarity of TSSCS found in the current study is that binocular-driven neurons mediate these aftereffects.

Our last finding, namely that TSSCS depends on the surround-to-center contrast ratio, is consistent with the effect of the texture surround being one of divisive inhibition (Krause & Pack, 2014; Nurminen & Angelucci, 2014; Schwabe, Ichida, Shushruth, Mangapathy, & Angelucci, 2010). It is also consistent with similar findings from the tilt illusion (Durant & Clifford, 2006; Qiu et al., 2013; Tolhurst & Thompson, 1975).

Conclusion

The selectivities shown here for luminance polarity and contrast in the context of interactions between contour-shape and texture-shape perception are consistent with one aim of vision being to segregate contours that define objects from those that form textured surfaces. It has been suggested that TSSCS is likely mediated by extraclassical receptive field neurons in early visual areas such as V1 that feed forward their responses into shape-selective neurons in intermediate-to-higher visual areas (Gheorghiu et al., 2014). Thus, the selectivity of TSSCS to luminance polarity and contrast may constitute an important neural substrate underlying efficient figure (object)–ground (texture) segregation and image segmentation.

Keywords: shape, contour, texture, surround suppression, luminance polarity, contrast, aftereffects

Acknowledgments

This research was supported by a Leverhulme Trust grant (RPG-2016-056) awarded to EG. Conceived and designed the experiments: EG, FK. Performed the experiments: EG. Analyzed the data: EG. Wrote the paper: EG, FK. The authors declare no competing interests.

Commercial relationships: none.
Corresponding author: Elena Gheorghiu.
Email: elena.gheorghiu@stir.ac.uk.
Address: University of Stirling, Department of Psychology, Stirling, Scotland, United Kingdom.

References

Bell, J., Gheorghiu, E., Hess, R. F., & Kingdom, F. A. (2011). Global shape processing involves a hierarchy of integration stages. *Vision Research*, *51*(15), 1760–1766.

Biederman, I. (1987). Recognition-by-components: A theory of human image understanding. *Psychological Review*, *94*(2), 115–147.

Blake, R., Overton, R., & Lema-Stern, S. (1981). Interocular transfer of visual aftereffects. *Journal of Experimental Psychology: Human Perception and Performance*, *7*(2), 367–381.

Blakemore, C., & Sutton, P. (1969, October 10). Size adaptation: A new aftereffect. *Science*, *166*(3902), 245–247.

Bonds, A. B. (1989). Role of inhibition in the specification of orientation selectivity of cells in the cat striate cortex. *Visual Neuroscience*, *2*(1), 41–55.

Bonds, A. B. (1991). Temporal dynamics of contrast gain in single cells of the cat striate cortex. *Visual Neuroscience*, *6*(3), 239–255.

Burton, G. J., Nagshineh, S., & Ruddock, K. H. (1977). Processing by the human visual system of the light

and dark contrast components of the retinal image. *Biological Cybernetics*, *27*(4), 189–197.

Chubb, C., Econopouly, J., & Landy, M. S. (1994). Histogram contrast analysis and the visual segregation of IID textures. *Journal of the Optical Society of America A*, *11*(9), 2350–2374.

De Valois, K. K. (1977a). Independence of black and white: Phase-specific adaptation. *Vision Research*, *17*(2), 209–215.

De Valois, K. K. (1977b). Spatial frequency adaptation can enhance contrast sensitivity. *Vision Research*, *17*(9), 1057–1065.

Durant, S., & Clifford, C. W. (2006). Dynamics of the influence of segmentation cues on orientation perception. *Vision Research*, *46*(18), 2934–2940.

Ehrenstein, W. H., & Spillmann, L. (1983). Time thresholds for increments and decrements in luminance. *Journal of the Optical Society of America A*, *73*(4), 419–426.

Fiorentini, A., Baumgartner, G., Magnussen, S., Schiller, P. H., & Thomas, J. P. (1990). The perception of brightness and darkness: Relations to neuronal receptive fields. In L. Spillmann & J. S. Werner (Eds.), *Visual perception: The neurophysiological foundations* (pp. 129–161). San Diego, CA: Academic Press.

Forte, J. D., & Clifford, C. W. (2005). Inter-ocular transfer of the tilt illusion shows that monocular orientation mechanisms are colour selective. *Vision Research*, *45*(20), 2715–2721.

Gheorghiu, E., Bell, J., & Kingdom, F. A. (2013). Line orientation adaptation: Local or global? *PLoS One*, *8*(8):e73307.

Gheorghiu, E., & Kingdom, F. A. (2006). Luminance-contrast properties of contour-shape processing revealed through the shape-frequency after-effect. *Vision Research*, *46*(21), 3603–3615.

Gheorghiu, E., & Kingdom, F. A. (2008). Spatial properties of curvature-encoding mechanisms revealed through the shape-frequency and shape-amplitude after-effects. *Vision Research*, *48*(9), 1107–1124.

Gheorghiu, E., & Kingdom, F. A. (2009). Multiplication in curvature processing. *Journal of Vision*, *9*(2): 23, 1–17, https://doi.org/10.1167/9.2.23. [PubMed] [Article]

Gheorghiu, E., & Kingdom, F. A. A. (2011). Spatial-properties of texture-surround suppression of contour-shape coding. *Journal of Vision*, *11*(11): 1038, https://doi.org/10.1167/11.11.1038. [Abstract]

Gheorghiu, E., & Kingdom, F. A. (2012a). Chromatic properties of texture-shape and of texture-surround suppression of contour-shape mechanisms. *Journal of Vision*, *12*(6):16, 1–17, https://doi.org/10.1167/12.6.16. [PubMed] [Article]

Gheorghiu, E., & Kingdom, F. A. (2012b). Local and global components of texture-surround suppression of contour-shape coding. *Journal of Vision*, *12*(6): 20, 1–19, https://doi.org/10.1167/12.6.20. [PubMed] [Article]

Gheorghiu, E., & Kingdom, F. A. (2017). Dynamics of contextual modulation of perceived shape in human vision. *Scientific Reports*, *7*:43274, https://doi.org/10.1038/srep43274.

Gheorghiu, E., Kingdom, F. A., Bell, J., & Gurnsey, R. (2011). Why do shape aftereffects increase with eccentricity? *Journal of Vision*, *11*(14):18, 1–21, https://doi.org/10.1167/11.14.18. [PubMed] [Article]

Gheorghiu, E., Kingdom, F. A., & Petkov, N. (2014). Contextual modulation as de-texturizer. *Vision Research*, *104*, 12–23.

Gheorghiu, E., Kingdom, F. A., Thai, M. T., & Sampasivam, L. (2009). Binocular properties of curvature-encoding mechanisms revealed through two shape after-effects. *Vision Research*, *49*(14), 1765–1774.

Gheorghiu, E., Kingdom, F. A., & Witney, E. (2010). Size and shape after-effects: Same or different mechanism? *Vision Research*, *50*(21), 2127–2136.

Graham, N. V. (2011). Beyond multiple pattern analyzers modeled as linear filters (as classical V1 simple cells): Useful additions of the last 25 years. *Vision Research*, *51*(13), 1397–1430.

Grigorescu, C., Petkov, N., & Westenberg, M. A. (2003). Contour detection based on nonclassical receptive field inhibition. *IEEE Transactions on Image Processing*, *12*(7), 729–739.

Grigorescu, C., Petkov, N., & Westenberg, M. A. (2004). Contour and boundary detection improved by surround suppression of texture edges. *Image and Vision Computing*, *22*(8), 609–622.

Hansen, B. C., & Hess, R. F. (2006). The role of spatial phase in texture segmentation and contour integration. *Journal of Vision*, *6*(5):5, 594–615, https://doi.org/10.1167/6.5.5. [PubMed] [Article]

He, Z. J., & Ooi, T. L. (1998). Illusory-contour formation affected by luminance contrast polarity. *Perception*, *27*(3), 313–335.

Heeger, D. J. (1992). Normalization of cell responses in cat striate cortex. *Visual Neuroscience*, *9*(2), 181–197.

Julesz, B. (1981, March 12). Textons, the elements of

texture perception, and their interactions. *Nature*, *290*(5802), 91–97.

Kingdom, F. A., & Prins, N. (2009). Texture-surround suppression of contour-shape coding in human vision. *Neuroreport*, *20*(1), 5–8.

Kingdom, F. A., Prins, N., & Hayes, A. (2003). Mechanism independence for texture-modulation detection is consistent with a filter-rectify-filter mechanism. *Visual Neuroscience*, *20*(1), 65–76.

Komban, S. J., Alonso, J. M., & Zaidi, Q. (2011). Darks are processed faster than lights. *Journal of Neuroscience*, *31*(23), 8654–8658.

Komban, S. J., Kremkow, J., Jin, J., Wang, Y., Lashgari, R., Li, X., ... Alonso J. M., (2014). Neuronal and perceptual differences in the temporal processing of darks and lights. *Neuron*, *82*(1), 224–234.

Krause, M. R., & Pack, C. C. (2014). Contextual modulation and stimulus selectivity in extrastriate cortex. *Vision Research*, *104*, 36–46.

Landy, M. S. (2013). Texture analysis and perception. In J. S. Werner & L. M. Chalupa (Eds.), *The New Visual Neurosciences* (pp. 639–652). Cambridge, MA: MIT Press.

Li, A., & Zaidi, Q. (2000). Perception of three-dimensional shape from texture is based on patterns of oriented energy. *Vision Research*, *40*(2), 217–242.

Li, Z. (1999). Visual segmentation by contextual influences via intra-cortical interactions in the primary visual cortex. *Network*, *10*(2), 187–212.

Li, Z. (2002). A saliency map in primary visual cortex. *Trends in Cognitive Sciences*, *6*(1), 9–16.

Magnussen, S., & Kurtenbach, W. (1979). A test for contrast-polarity selectivity in the tilt aftereffect. *Perception*, *8*(5), 523–528.

Malik, J., & Perona, P. (1990). Preattentive texture discrimination with early vision mechanisms. *Journal of the Optical Society of America A*, *7*(5), 923–932.

Marr, D. (1982). From images to surfaces. In *Vision: A computational investigation into the human representation and processing of visual information* (pp. 215–239). San Francisco, CA: W. H. Freeman.

Motoyoshi, I., & Kingdom, F. A. A. (2007). Differential roles of contrast polarity reveal two streams of second-order visual processing. *Vision Research*, *47*(15), 2047–2054.

Nurminen, L., & Angelucci, A. (2014). Multiple components of surround modulation in primary visual cortex: Multiple neural circuits with multiple functions? *Vision Research*, *104*, 47–56.

Ohzawa, I., Sclar, G., & Freeman, R. D. (1982, July 15). Contrast gain control in the cat visual cortex. *Nature*, *298*(5871), 266–268.

Ohzawa, I., Sclar, G., & Freeman, R. D. (1985). Contrast gain control in the cat's visual system. *Journal of Neurophysiology*, *54*(3), 651–667.

Petkov, N., & Westenberg, M. A. (2003). Suppression of contour perception by band-limited noise and its relation to nonclassical receptive field inhibition. *Biological Cybernetics*, *88*(3), 236–246.

Prins, N., & Kingdom, F. A. A. (2002). Orientation- and frequency-modulated textures at low depths of modulation are processed by off-orientation and off-frequency texture mechanisms. *Vision Research*, *42*, 705–713.

Qiu, C., Kersten, D., & Olman, C. A. (2013). Segmentation decreases the magnitude of the tilt illusion. *Journal of Vision*, *13*(13):19, 1–17, https://doi.org/10.1167/13.13.19. [PubMed] [Article]

Rekauzke, S., Nortmann, N., Staadt, R., Hock, H. S., Schoner, G., & Jancke, D. (2016). Temporal asymmetry in dark-bright processing initiates propagating activity across primary visual cortex. *Journal of Neuroscience*, *36*(6), 1902–1913.

Rentschler, I., Hubner, M., & Caelli, T. (1988). On the discrimination of compound Gabor signals and textures. *Vision Research*, *28*(2), 279–291.

Schwabe, L., Ichida, J. M., Shushruth, S., Mangapathy, P., & Angelucci, A. (2010). Contrast-dependence of surround suppression in macaque V1: Experimental testing of a recurrent network model. *Neuroimage*, *52*(3), 777–792.

Shi, L., & Shinomori, K. (2013). Amplitude difference and similar time course of impulse responses in positive- and negative-contrast detection. *Vision Research*, *77*, 21–31.

Sutter, A., Sperling, G., & Chubb, C. (1995). Measuring the spatial frequency selectivity of second-order texture mechanisms. *Vision Research*, *35*(7), 915–924.

Suzuki, S. (2001). Attention-dependent brief adaptation to contour orientation: A high-level aftereffect for convexity? *Vision Research*, *41*(28), 3883–3902.

Tolhurst, D. J., & Thompson, P. G. (1975). Orientation illusions and after-effects: Inhibition between channels. *Vision Research*, *15*, 967–972.

Whittle, P. (1986). Increments and decrements: Luminance discrimination. *Vision Research*, *26*(10), 1677–1691.

Xing, D., Yeh, C. I., & Shapley, R. M. (2010). Generation of black-dominant responses in V1

cortex. *Journal of Neuroscience*, *30*(40), 13504–13512.

Yamashita, J. A., Hardy, J. L., De Valois, K. K., & Webster, M. A. (2005). Stimulus selectivity of figural aftereffects for faces. *Journal of Experimental Psychology: Human Perception and Performance*, *31*(3), 420–437.

Supplementary material

Supplementary Movie S1. Example dynamic stimuli used in the experiments. Dynamic version of the shape-frequency aftereffect obtained with contour adaptor and contour test. An important property of the shape aftereffect is that it survives shape-phase randomization during adaptation.